J. Fluid Mech. (2009), *vol.* 621, *pp.* 243–258.
doi:10.1017/S0022112008004746 Printed in the United Kingdom

Impact of a rising stream on a horizontal plate of finite extent

P. CHRISTODOULIDES[1] AND F. DIAS[2]†

[1]Faculty of Engineering and Technology, Cyprus University of Technology, Limassol, Cyprus

[2]CMLA, ENS Cachan and CNRS, UniverSud, 61 avenue du President Wilson, F-94235 Cachan Cedex, France

(Received 8 July 2008 and in revised form 16 October 2008)

The steady flow of a stream emerging from a nozzle, hitting a horizontal plate and falling under gravity is considered. Depending on the length of the plate L and the Froude number F, the plate can either divert the stream or lead to its detachment. First, the problem is reformulated using conformal mappings. The resulting problem is then solved by a collocation Galerkin method; a particular form is assumed for the solution, and certain coefficients in that representation are then found numerically by satisfying Bernoulli's equation on the free surfaces at certain discrete points. The resulting equations are solved by Newton's method, yielding various configurations of the solution based on the values of F and L. The lift exerted on the plate is computed and discussed. If the plate is long enough, physically meaningful solutions are found to exist only for values of F greater than or equal to a certain critical value F_0, which is to be determined. Results are presented, both for $F > F_0$ where the detachment is horizontal and for $F = F_0$ where the detachment point is a stagnation point at a 120° corner. Related asymmetric flows where the rising stream is inclined are also studied.

1. Introduction

Rising flows occur in numerous applications. For example, water fountains have a long history, as thoroughly described by Clanet (1998). While Clanet's study was experimental, several papers have been devoted to numerical computations of flows emerging from a nozzle and falling under gravity. The numerical computation of free-surface flows in the presence of gravity is a notoriously difficult problem. There is an extended literature on jets impinging on obstacles of various shapes in the absence of gravity (see, for example, Hureau, Brunon & Legallais 1996 or Peng & Parker 1997). This is why we restrict our literature review on free-surface flows in the presence of gravity. Dias & Vanden-Broeck (1990) studied a steady stream splitting into two sheet-like jets. Dias & Christodoulides (1991) studied a rising stream which falls down as a single jet as it escapes from the nozzle. Vanden-Broeck & Keller (1982) considered steady jets, rising and falling under gravity. Dias & Vanden-Broeck (1993) considered bow flows with a jet in front of the ship. Vanden-Broeck (1993) investigated jets aimed vertically upwards without the presence of any solid boundaries. An interesting limiting case of the nozzle problem is obtained when the nozzle is horizontal. The corresponding configuration is known as the waterfall problem (see, for example, Goh & Tuck 1985 or Dias & Tuck 1991). A variant of this

† Email address for correspondence: dias@cmla.ens-cachan.fr

problem is the flow of a stream of water falling under gravity after emerging from a simple slit orifice in a vertical wall (see Tuck 1987). Wiryanto & Tuck (2000) also considered the flow in a channel which ends abruptly with a barrier in the form of a vertical wall of finite height. Hence, the stream is forced to go upward and then falls under the effect of gravity. The present study gives insight to a realistic case which, to our knowledge, has not been studied yet: the case where a plate diverts the jet emerging from a nozzle pointing upward. The results obtained in this paper could be used, for example, to control jets, in particular their direction, by positioning a plate higher or lower relative to the nozzle. Several limiting cases are discussed as well.

A stream of fluid flows up and out of the top of a long two-dimensional vertically sided pipe of half-width W. The upwardly directed flow meets a horizontal plate of half-length L set at a height H above the top of the pipe (if the nozzle is wider than the plate, the plate can be put inside the nozzle as well and then H becomes negative). The flow splits into two jets that reach a maximum height on each side of the plate and then fall under gravity. The solution depends on H/W, L/W and on the dimensionless Froude number

$$F = \frac{U}{\sqrt{gW}}, \tag{1.1}$$

where g is the acceleration due to gravity and U the velocity of the fluid far inside the nozzle.

The problem is formulated in § 2. Since the flows are two-dimensional, one can use the theory of functions of a complex variable. Conformal mappings lead to a formulation of the problem that is well suited for discretization. A system of N nonlinear equations in N unknowns is then derived. The problem is solved numerically through a collocation Galerkin method explained in § 3. The numerical results and some computed profiles of the free surfaces are presented in § 4. A study of the lift force exerted on the horizontal plate and of the pressure distribution along the plate is performed in § 5. In § 6 we study related flows where the detachment point along the plate is a stagnation point and in § 7 we extend our study to the case of a stream emerging from a nozzle and splitting into two non-symmetric jets, without hitting the horizontal plate. In fact, one may regard this special configuration as the case where the plate is too high to be hit. Finally, we consider cases where the nozzle is inclined at an angle β of elevation to the positive horizontal axis.

2. Formulation of the problem

We consider the steady irrotational flow of an incompressible inviscid fluid emerging from a nozzle of width $2W$ directed upward, hitting a horizontal plate of length $2L$ placed at a vertical distance H from the edges of the nozzle (this distance H can be negative if the plate is narrower than the nozzle), and falling symmetrically under gravity. As shown in figure 1(a), the stream coming from far inside the nozzle (see point I) hits the horizontal plate, centred at point A, and forms two jets – one on each side – detaching at points $B(B')$ and $S(S')$ and forming free surfaces $B \to J(B' \to J')$ and $S \to J(S' \to J')$ to the right (left).

Due to symmetry, the formulation of the problem is based on the 'right' half of the flow. The results presented in the sequel are simply obtained by superposition of the 'left' and 'right' flows. The coordinate system to be used is (x, y), x being horizontal and y vertical. The point B is taken as the origin. The mass flux emerging from the

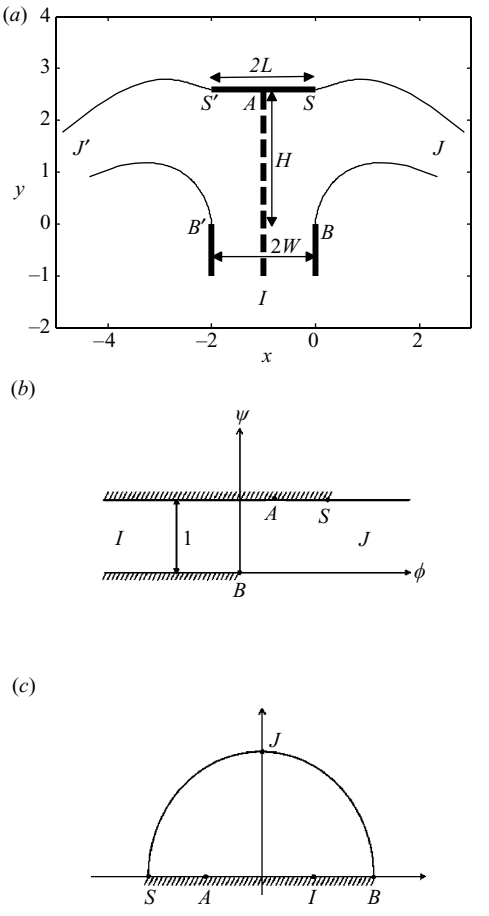

FIGURE 1. (*a*) Sketch of the flow and of the coordinates. The free-surface profile is a computed solution for $F = 2.0$ and $(x_S,\ y_S) = (0, 2.6)$. Special points are labelled on the boundary. (*b*) The complex potential f-plane. The images of the special points are shown. (*c*) The complex t-plane. The images of the special points are shown.

'right' nozzle is

$$Q = UW. \tag{2.1}$$

Let u and v denote the x- and y-components of the fluid velocity. The system is governed by the assumptions of irrotationality and incompressibility, which leads to $(u, v) = \nabla\phi$ with Laplace's equation $\nabla^2\phi = 0$ holding for the velocity potential ϕ; Bernoulli's equation then follows as a first integral of the Euler (momentum) equations of motion. It reads

$$\frac{1}{2}(u^2 + v^2) + gy + \frac{p}{\rho} = \text{constant}, \tag{2.2}$$

which is valid everywhere inside the fluid and where p is the pressure and ρ the fluid density. Assuming that the pressure has the same constant value $p = 0$ on all free surfaces, and taking W and U as the unit length and unit velocity respectively, Q becomes unity and Bernoulli's equation on the free surfaces becomes, in dimensionless

form,

$$\frac{1}{2}(u^2+v^2)+\frac{1}{F^2}y=\frac{1}{2}v_B^2, \tag{2.3}$$

where the same symbols are kept for the dimensionless variables for the sake of simplicity. The constant on the right-hand side has been evaluated at point B, where the velocity is purely vertical and $y=0$.

The problem under consideration can be solved with the use of conformal mappings. Hence, we define the complex variable $z=x+\mathrm{i}y$ and the complex potential $f=\phi+\mathrm{i}\psi$, for the velocity potential $\phi(x,y)$ and the streamfunction $\psi(x,y)$. Then we also introduce the hodograph variable

$$\zeta(z)\equiv\frac{\mathrm{d}f}{\mathrm{d}z}=u-\mathrm{i}v. \tag{2.4}$$

The flow domain in the f-plane is represented in figure 1(b). It lies within an infinite strip of height 1. Without loss of generality the point B is taken as the origin of the complex potential.

We then transform the domain of the fluid in the f-plane into the upper half of the unit disk in the t-plane so that points S, J and B are mapped into points –1, i and 1 respectively, as shown in figure 1(c). The 'left' side of the half-nozzle goes onto $[t_A, t_I]$ and the 'right' side onto $[t_I, 1]$, while the horizontal plate goes onto $[-1, t_A]$, with the upper free surface going onto the left quarter of the half-circle and the lower free surface onto the right quarter of the half-circle. The transformation from the f-plane to the t-plane can be written in differential form as

$$\frac{\mathrm{d}f}{\mathrm{d}t}=\frac{1}{\pi}\left(1+t_I^2\right)\frac{1-t^2}{(1+t^2)(t-t_I)(1-tt_I)} \tag{2.5}$$

or in integrated form as

$$f=\frac{1}{\pi}\ln\left(\frac{2(t-t_I)(1-tt_I)}{(1-t_I)^2(1+t^2)}\right). \tag{2.6}$$

The free surfaces in the t-plane are described by the points $t=\mathrm{e}^{i\sigma}$, $\sigma\in[0,\pi]$. Clearly, one can obtain t as a function of f explicitly by inverting relation (2.6).

The problem now reduces to finding the hodograph variable ζ as an analytic function of t, satisfying Bernoulli's equation (2.3) on the free surfaces and the kinematic boundary condition on the real diameter $t\in[-1,1]$.

The following singularities are present.

(i) At point A, the velocity of the fluid vanishes and the appropriate behaviour for ζ is given by

$$\zeta\sim(t-t_A)^{1/2}\quad\text{as}\quad t\to t_A. \tag{2.7}$$

(ii) At point J, there is a jet-type singularity and the appropriate behaviour for ζ is given by

$$\zeta\sim[\ln(1+t^2)]^{1/3}\quad\text{as}\quad t\to\mathrm{i}. \tag{2.8}$$

(For more details on these singularities, see for example Vanden-Broeck & Keller 1986.) It is then possible to define the function $\Omega(t)$ by the relation

$$\zeta(t)=-\mathrm{i}\frac{(t-t_A)^{1/2}[-\ln c(1+t^2)]^{1/3}\mathrm{e}^{\Omega(t)}}{(t_I-t_A)^{1/2}\left[-\ln c\left(1+t_I^2\right)\right]^{1/3}\mathrm{e}^{\Omega(t_I)}}, \tag{2.9}$$

where $|\zeta(t_I)| = 1$. The function $\Omega(t)$ is analytic for $|t| < 1$ and continuous for $|t| \leqslant 1$, and can be expanded in a power series of the form

$$\Omega(t) = \sum_{n=1}^{\infty} a_n t^n. \tag{2.10}$$

The constant c in (2.9) is chosen such that all cube-roots in (2.9) are positive for $t \in (-1, 1)$ and do not vanish for $t = 0$. A good choice is $c = 0.2$. The value of ζ does not depend on c but the values of the coefficients a_n do.

3. Numerical method

The coefficients a_n in the power series (2.10) can be determined by using a collocation Galerkin method. We truncate the infinite series after $N - 2$ terms and introduce on the free surfaces the $N - 2$ mesh points

$$\sigma_M = \frac{\pi}{N-2}\left(M - \tfrac{1}{2}\right), \quad M = 1, \ldots, N-2. \tag{3.1}$$

To compute the values of y in Bernoulli's equation (2.3), use is made of the equation

$$\frac{\mathrm{dz}}{\mathrm{dt}} = \frac{1}{\zeta}\frac{\mathrm{df}}{\mathrm{dt}}, \tag{3.2}$$

which is integrated numerically. Substituting the expressions of y and ζ into equation (2.3) at the mesh points σ_M, we obtain $N - 2$ nonlinear algebraic equations for the N unknowns $a_1, \ldots, a_{N-2}$, t_I and t_A. The last two equations are obtained by imposing the position of point S. In other words, we impose the extent of the horizontal plate x_S and the vertical aperture y_S between the plate and the nozzle.

This system of N nonlinear equations in N unknowns is solved by Newton's method for given values of the Froude number F using MATLAB. All the computations were performed with $N = 200$, after a check on accuracy was performed. Typical orders of magnitude for a_1, a_{20} and a_{100} are $|a_1| \approx 10^{-1}$, $|a_{20}| \approx 10^{-2}$ and $|a_{100}| \approx 10^{-3}$.

To summarize, the solutions we consider form a three-parameter family of solutions. The three parameters are the Froude number F given by (1.1), the offset parameter x_S equal to $L/W - 1$ and the aperture parameter y_S equal to H/W. The theoretical ranges of these three parameters are

$$F \in (0, \infty), \quad x_s \in (-1, \infty), \quad y_s \begin{cases} (0, \infty) & \text{if} \quad x_S > 0 \\ (-\infty, \infty) & \text{if} \quad x_S < 0. \end{cases}$$

When the offset is negative ($x_S < 0$) one obtains underhanging configurations, while for positive offsets ($x_S > 0$) one obtains overhanging configurations. When $x_S = 0$, the edge of the plate is on the same vertical line as the side of the nozzle. Of course, if the elevation of the plate is too high, the flow may not reach the plate, so there is an upper bound on y_S. Finally, if the nozzle is wider than the plate ($x_S < 0$), the plate can be put inside the nozzle (with $y_S < 0$). But again if the plate is too deep inside the nozzle, the flow will not be able to escape and so there is also a lower bound on y_S.

4. Numerical results

Before we describe the numerical results, we briefly consider the limiting case without gravity ($F \to \infty$) and with infinite offset ($x_S \to \infty$). Then there is only one

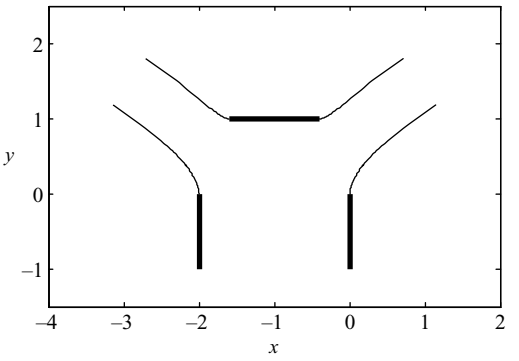

FIGURE 2. Same as figure 1(*a*) for $F = 2.0$ and $(x_S, y_S) = (-0.4, 1.0)$. We refer to such flows as 'rising' jets.

parameter left, aperture y_S. This particular case was considered in the monograph by Milne-Thomson (1996, Example XII.10 and figure 14.8*b*), where an analytical solution was provided. For example, one has the following explicit relation between y_S and the ultimate width $d = D/W$ of the jet in contact with the plate (W being the (horizontal) width of the jet in the nozzle and D being the far-field (vertical) depth of the stream of fluid on the underside of the horizontal plate):

$$y_S = d + \frac{1+d^2}{\pi} \ln\left(\frac{1+d}{1-d}\right). \tag{4.1}$$

As y_S increases from 0 to ∞, d increases monotonically from 0 to 1. The solution for the limiting case ($F \to \infty$, $x_S \to \infty$) looks like the solution shown in figure 3, with the plate extended to infinity and the lower free surface staying horizontal at infinity.

In order to study systematically the three-parameter family of solutions, we let the offset of the plate and the aperture between plate and nozzle (in other words, the coordinates x_S and y_S of the point S) vary for given values of the Froude number F. One way to classify the solutions into three types of flows is as follows. Imagine that the Froude number F is fixed and that one varies the size and the position of the plate. If the plate is short enough and not too high, the flow will continue as two rising jets, after hitting the plate. If the plate is long enough, the flow will follow the plate without rising any longer. It will eventually develop into two downward jets. If the plate is neither short nor long, the flow will look like a fountain (see figure 1*a*).

We now present results – covering all cases – for $F = 2.0$. More computations have been performed at other Froude numbers, but it was found that the general behaviour is the same. Results with the whole range of Froude numbers will be given in § 6.

(a) *Rising* jet. In this case, the stream is weakly diverted by the horizontal plate when hitting it and then continues to rise in the form of jets before eventually falling down under gravity. This is shown in figure 2 for $(x_S, y_S) = (-0.4, 1.0)$.

(b) *Overhanging* jet. In this case, the stream is strongly diverted by the horizontal plate when hitting it and then follows an almost horizontal trajectory in the form of jets before eventually falling down under gravity. This is shown in figure 3 for $(x_S, y_S) = (1.3, 1.1)$. Using $y_S = 1.1$, one can use (4.1) to compute the ultimate width that the jet would reach if the Froude number was infinite and the plate infinitely long. One finds $d = 0.564$. This value can be compared with the width of the jet as it leaves the plate at $x = x_S$. One finds a thickness equal to 0.615, which is within 10 % of the no-gravity value.

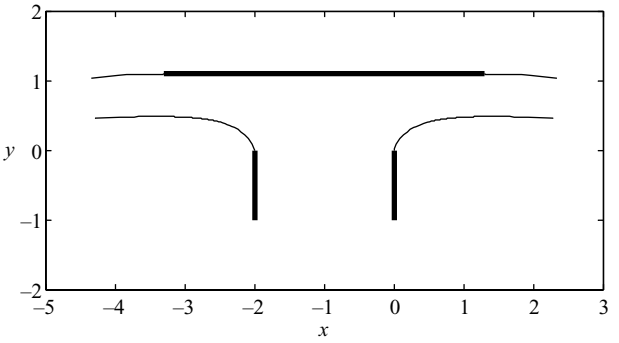

FIGURE 3. Same as figure 1(*a*) for $F = 2.0$ and $(x_S, y_S) = (1.3, 1.1)$. We refer to such flows as 'overhanging' jets.

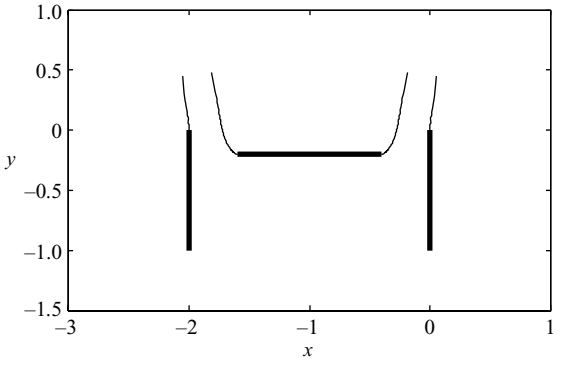

FIGURE 4. Free-surface profiles for a plate placed inside the nozzle. The parameter values are $F = 2.0$ and $(x_S, y_S) = (-0.4, -0.2)$.

(c) *Intermediate* jet. In this case, the stream rises slightly after hitting the plate, but then quickly falls down under gravity. An example was already shown in figure 1(*a*) for $(x_S, y_S) = (0, 2.6)$. The flow looks like a fountain and the plate has only a small effect on the flow.

If the nozzle is wider than the plate, the plate can be put inside the nozzle. An example of such flow, with rising jets, is shown in figure 4.

5. Uplift force exerted on the horizontal plate

The lift F_L exerted on the plate is evaluated. It is equal to the vertical component of the pressure force exerted on the plate (since the plate is horizontal, there is in fact no horizontal component). Using Bernoulli's equation (2.2), one obtains the following expression for the lift coefficient C_L:

$$C_L = \frac{F_L}{\frac{1}{2}\rho U^2 L} = \frac{W}{L}\int_{-1}^{x(S)} \frac{p}{\frac{1}{2}\rho U^2}\,\mathrm{d}x = \frac{1}{1+x(S)}\int_{-1}^{x(S)} \left(u_S^2 - u^2 - v^2\right)\mathrm{d}x, \qquad (5.1)$$

where p is the physical pressure and u_S the velocity at the edge of the plate (point S). Since the flows depend on three independent parameters (F, x_S and y_S), it is not possible to perform a full parametric study. It was decided to fix the Froude number and let the elevation of the plate y_S vary for a discrete set of values of the offset x_S, the plate half-length being $1 + x_S$. Results are presented in figure 5. For some

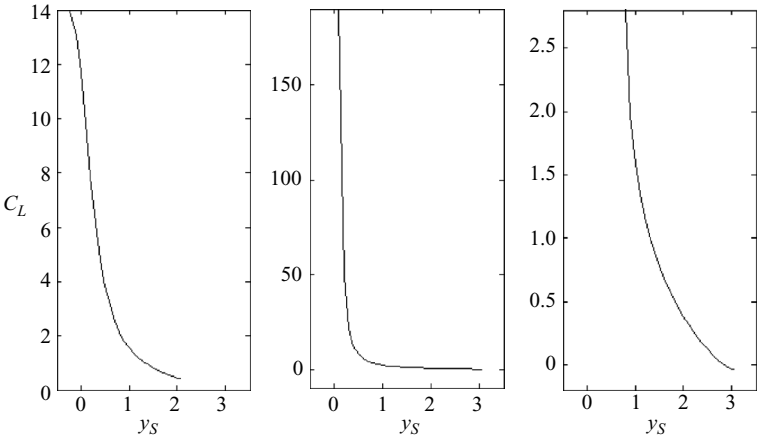

FIGURE 5. Lift exerted on the plate. Plot of the lift coefficient (5.1) as a function of the plate-elevation y_S, for three different values of the offset x_S, for $F=2$. Left: $x_S=-0.4$; middle: $x_S=0$; right: $x_S=1.3$. For the case on the left (negative offset), the plate can be placed inside the nozzle and y_S can be negative. Note the different vertical scales on the middle and right plots: the lift coefficient on the right plot increases so rapidly as y_S tends to zero that only the small values of C_L are shown.

parameters, the lift coefficient was found to be negative (see the middle and right plots). In other words, the plate is being sucked down by the flow rather than being lifted up. This somewhat counterintuitive result can be explained as follows. Along the plate $S'AS$, Bernoulli's equation simply reads

$$\tfrac{1}{2}u^2 + p = \tfrac{1}{2}u_S^2.$$

At the centre of the plate (point A) the pressure is maximum since the velocity u is 0. At the edges of the plate (points S' and S) the pressure is 0 (atmospheric pressure). In the limit as point S becomes a stagnation point (see § 6), the velocity u_S becomes identically 0 and therefore the pressure must be negative everywhere along the plate ($p=-1/2u^2$). On the middle and right plots, the upper bound for y_S indeed corresponds to the formation of a stagnation point at the edge of the plate S. On the left plot, the computations were stopped at a value of y_S slightly above 2 because a stagnation point began to form on the upper free surface away from the plate edge.

Various pressure profiles along the plate are given in figure 6. They correspond to the three cases described in § 4 (rising jet, overhanging jet, intermediate jet). In addition, we show an example with both positive and negative pressures along the plate. The pressures have been non-dimensionalized by $1/2\rho U^2$.

6. Flows with a stagnation point

If one wishes to impose the condition that the edges of the horizontal plate S and S' are stagnation points, then – following the formulation in § 2 – there will be an extra singularity in the complex velocity in addition to the singularities at points A and J already defined in (2.7) and (2.8). Repeating here these singularities for convenience,

(i) $\zeta \sim (t-t_A)^{1/2}$ as $t \to t_A$,

(ii) $\zeta \sim [\ln(1+t^2)]^{1/3}$ as $t \to \mathrm{i}$,

one adds the following singularity:

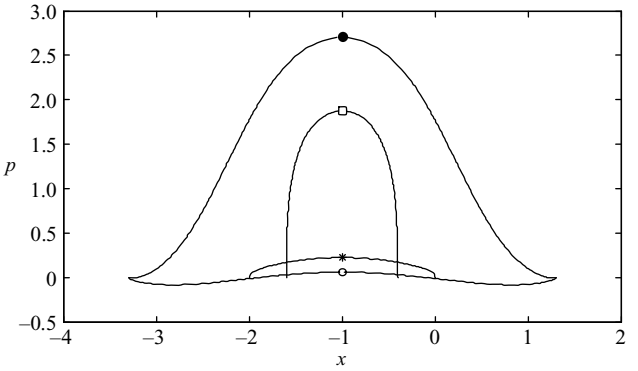

FIGURE 6. Four different pressure profiles along the plate for $F = 2$. The pressure is non-dimensionalized by $1/2\rho U^2$. The labels are ●, $(x_S, y_S) = (1.3, 1.1)$; □, $(x_S, y_S) = (-0.4, 1.0)$; *, $(x_S, y_S) = (0, 2.6)$; ○, $(x_S, y_S) = (1.3, 2.9)$.

(iii) At point S, the velocity of the fluid vanishes and the appropriate behaviour for ζ is given by

$$\zeta \sim (t+1)^{2/3} \quad \text{as} \quad t \to -1. \tag{6.1}$$

It is then possible to define the function $\Omega(t)$ by the relation

$$\zeta(t) = -\mathrm{i}\frac{(1+t)^{2/3}(t-t_A)^{1/2}\big[-\ln c(1+t^2)\big]^{1/3}\mathrm{e}^{\Omega(t)}}{(1+t_I)^{2/3}(t_I-t_A)^{1/2}\big[-\ln c(1+t_I^2)\big]^{1/3}\mathrm{e}^{\Omega(t_I)}}, \tag{6.2}$$

where $|\zeta(t_I)| = 1$. We then truncate the infinite series (see (2.10)) after $N - 3$ terms and introduce on the free surfaces the $N - 2$ mesh points

$$\sigma_M = \frac{\pi}{N-2}\big(M - \tfrac{1}{2}\big), \qquad M = 1, \ldots, N-2. \tag{6.3}$$

Substituting the expressions of y and ζ into (2.3) at the mesh points σ_M, we obtain $N - 2$ nonlinear algebraic equations for the N unknowns $a_1, \ldots, a_{N-3}$, F, t_I and t_A. The last two equations are obtained by imposing the position of S.

This system of N nonlinear equations in N unknowns is solved by Newton's method using MATLAB. All the computations presented below were performed with $N = 200$, after a check on accuracy was performed.

We first study the effect of the position of the stagnation point S on the Froude number F. For three 'extreme' values of x_S, namely -0.95, 0 (the plate length and the nozzle width are equal) and 1, i.e. letting the horizontal plate vary from very short to long, the resulting relation F vs y_S is demonstrated in table 1. It turns out that the x-coordinate of the stagnation point has very little effect on the relation F vs y_S. Of interest is the fact that when $x_S = 1$ (long plate), there is a limiting plate elevation at about $y_S = 0.42$. If the plate is lowered below that value, the flow will not be able to reach the end of the plate and will detach before the edge of the plate. This limiting behaviour occurs for all positive values of x_S.

Figure 7 shows the computed solution for a long horizontal plate with $(x_S, y_S) = (1.0, 3.0)$, yielding $F = 1.959$. Finally, figure 8 shows the computed solution for a very short horizontal plate with $(x_S, y_S) = (-0.99, 1.64)$, yielding $F = 1.04$. This can be compared with the limiting case of no horizontal plate. In fact solutions of this kind (in the absence of horizontal plate) were computed by Dias & Christodoulides

$y_S \backslash\ x_S$	−0.95	0	1
0.1	0.019	0.018	–
0.2	0.053	0.052	–
0.3	0.096	0.094	–
0.4	0.147	0.144	–
0.42	0.159	0.155	0.205
0.5	0.204	0.200	0.265
0.6	0.267	0.261	0.338
0.8	0.402	0.394	0.488
1.0	0.547	0.538	0.636
1.2	0.699	0.688	0.781
1.4	0.852	0.841	0.923
1.6	1.005	0.994	1.063
1.8	1.155	1.145	1.201
2.0	1.302	1.293	1.337
2.2	1.445	1.437	1.470
2.4	1.583	1.577	1.600
2.5	1.650	1.645	1.664
2.7	1.781	1.776	1.788
2.8	1.844	1.840	1.849
3.0	1.966	1.963	1.959

TABLE 1. Values of the Froude number F as a function of x_S and y_S for flows with a stagnation point.

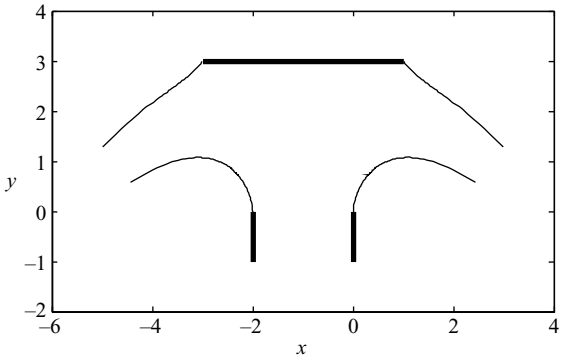

FIGURE 7. Free-surface profiles with stagnation point at $(x_S, y_S) = (1.0, 3.0)$. The Froude number $F = 1.96$ comes as part of the solution.

(1991). The solution here compares well with the solution presented in figure 3 of that paper.

Next, we study flows with low Froude numbers. We started by computing solutions without a stagnation point at point S. We fixed x_S and y_S, and let the Froude number decrease. Solutions were found to exist only for values of F greater than a certain critical value F_0. For example, with $(x_S, y_S) = (-0.68, 1.20)$, the critical value F_0 is roughly 0.70. Then we switched to the code with stagnation points at the plate edges, fixed $(x_S, y_S) = (-0.68, 1.20)$ and found F as part of the solution. Not surprisingly, the result was $F = F_0$. The free-surface profiles are shown in figure 9. We compared the free surfaces obtained with both codes (with and without stagnation at point S) and obtained excellent agreement, even near the singular point S. Even though the

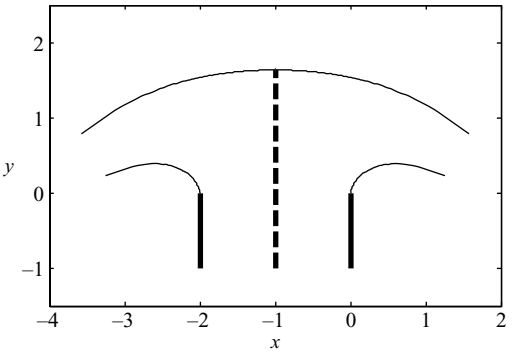

FIGURE 8. Free-surface profiles with stagnation point at $(x_S, y_S) = (-0.99, 1.64)$. The Froude number $F = 1.04$ comes as part of the solution. The plate is so small (total length of 0.02) that it cannot be seen in the figure. Points A (centre of the plate) and S (edge of the plate) are both stagnation points but they have different singular behaviour.

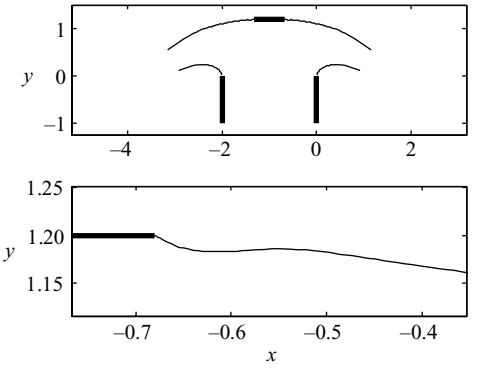

FIGURE 9. Free-surface profiles for $(x_S, y_S) = (-0.68, 1.20)$ and $F = 0.70$ and the blow-up of the upper right free surface near the stagnation point S.

expansions are different, the effect of the stagnation point is so local that it barely influences the whole flow. The flow shown in figure 9 looks similar to the weir flows computed by Vanden-Broeck & Keller (1987) and Dias, Keller & Vanden-Broeck (1988).

In figures 7–9, the stagnation points S and S' are precisely at the ends of the plate. The angles are of 120° and the plate can be arbitrarily extended to the left and to the right (with the plate dry) without changing the flow.

7. Flows emerging from an inclined nozzle in the absence of horizontal plate

As already mentioned in § 6, removing the horizontal plate – or equivalently letting its distance from the edges of the vertical nozzle go to infinity – reduces the problem to the vertical nozzle case studied by Dias & Christodoulides (1991). Here, however, we wish to study the case where there is no symmetry in the flow. Moreover, the nozzle can be inclined at an angle β of elevation to the positive horizontal axis. This is shown in figure 10(a), where the stream coming from far inside the nozzle (see point C) reaches a maximum (stagnation point S) and splits into two jets: one falling on the left of S forming a single free surface along the upper side of the nozzle (see

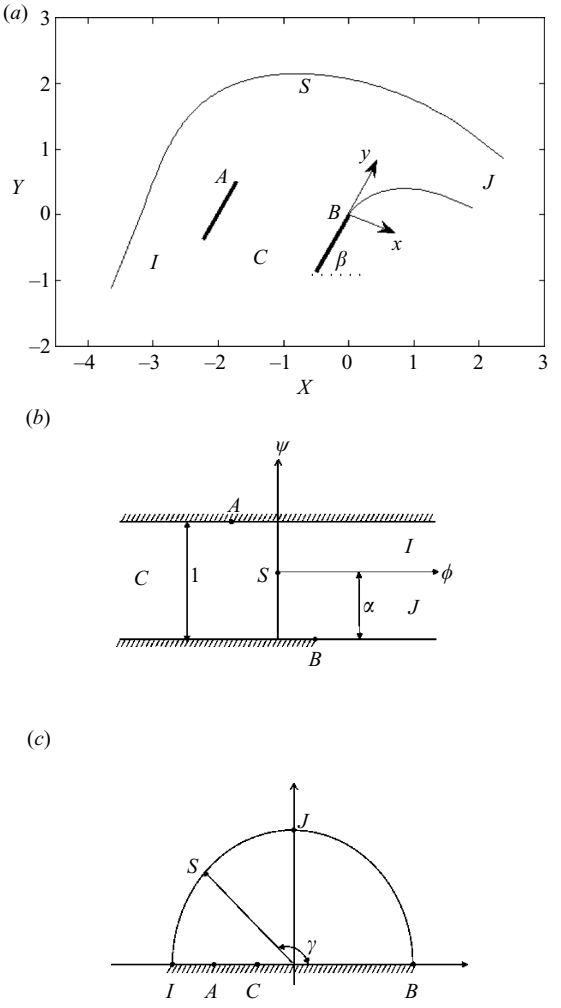

FIGURE 10. (*a*) Sketch of the flow. The free-surface profile is a computed solution for $\beta = 60^\circ$ and $F = 1.2$. The coordinates of the stagnation point S, $(X_S, Y_S) = (-0.80, 2.15)$, come as part of the solution. (*b*) The complex potential f-plane with the images of the special points. (*c*) The complex t-plane with the images of the special points.

$S \to I$), and one falling on the right of S forming two free surfaces pointing vertically downward (see $S \to J$ and $B \to J$).

For the numerical study of the flow, two systems of orthonormal coordinates are introduced: (X, Y), X being horizontal and Y being vertical, and (x, y), y being along the direction of the nozzle. In this section, we take the full width of the nozzle and the velocity of the fluid far inside the nozzle as unit length and unit velocity respectively. Therefore, the mass flux is again unity. However, all figures have been rescaled by a factor 2 for the sake of consistency with the rest of the paper.

The system is governed by Bernoulli's equation which in dimensionless form yields

$$\frac{1}{2}(u^2 + v^2) + \frac{1}{F^2}(y \sin\beta - x \cos\beta) = \text{constant on free surface.} \tag{7.1}$$

Now, the flow domain can be represented in the f-plane as in figure 10(b). We have an infinite strip of height 1. Without loss of generality the stagnation point S is taken as the origin of the complex potential.

We then transform the domain of the fluid in the f-plane into the upper half of the unit disk in the t-plane so that points I, J and B are mapped into points -1, i and 1 respectively, as shown in figure 10(c). The upper (left) side of the nozzle goes onto $[t_A, t_C]$ and the lower (right) side onto $[t_C, 1]$, with the upper free surface going onto the left quarter of the half-circle and the lower free surface onto the right quarter of the half-circle. The point S is mapped into $t_S = \mathrm{e}^{i\gamma}$. The transformation from the f-plane to the t-plane can be written in differential form as

$$\frac{\mathrm{d}f}{\mathrm{d}t} = \frac{1}{\pi}\left(\frac{(1+t_C)^2(1+t_C^2)}{(2t_C\cos\gamma - 1 - t_C^2)}\right)\left(\frac{(1-t)(2t\cos\gamma - 1 - t^2)}{(1+t)(1+t^2)(t-t_C)(1-tt_C)}\right) \tag{7.2}$$

or in integrated form as

$$f = \frac{2}{\pi}\frac{(1+t_C^2)(1+\cos\gamma)}{(2t_C\cos\gamma - 1 - t_C^2)}\ln\left(\frac{1+t}{2\cos\frac{1}{2}\gamma}\right) - \frac{1}{\pi}\frac{(1+t_C)^2\cos\gamma}{(2t_C\cos\gamma - 1 - t_C^2)}\ln\left(\frac{1+t^2}{2\cos\gamma}\right) + \frac{1}{\pi}\ln\left(\frac{(t-t_C)(tt_C-1)}{2t_C\cos\gamma - 1 - t_C^2}\right). \tag{7.3}$$

The free surfaces in the t-plane are described by the points $t = \mathrm{e}^{i\sigma}$, $\sigma \in [0, \pi]$. Also note that the proportion of the fluid volume flux going to the right is given by

$$\alpha = \frac{(1+t_C)^2\cos\gamma}{2t_C\cos\gamma - 1 - t_C^2}.$$

The following singularities are present.

At the edge A of the nozzle, the velocity of the fluid is infinite and the appropriate behaviour for ζ is

$$\zeta \sim (t - t_A)^{-1} \quad \text{as} \quad t \to t_A. \tag{7.4}$$

At the stagnation point S, the velocity vanishes and the appropriate behaviour for ζ is

$$\zeta \sim t - \mathrm{e}^{i\gamma} \quad \text{as} \quad t \to \mathrm{e}^{i\gamma},$$

or

$$\zeta \sim t^2 + 1 - 2t\cos\gamma \quad \text{as} \quad t \to \mathrm{e}^{i\gamma}. \tag{7.5}$$

Singularities at I and J are of jet-type and the appropriate behaviour for ζ is given respectively by

$$\zeta \sim [\ln(1+t)]^{1/3} \quad \text{as} \quad t \to -1 \tag{7.6}$$

and

$$\zeta \sim [\ln(1+t^2)]^{1/3} \quad \text{as} \quad t \to \mathrm{i}. \tag{7.7}$$

It is then possible to define the function $\Omega(t)$ by the relation

$$\zeta(t) = -\mathrm{i}\left(\frac{1+t^2-2t\cos\gamma}{1+t_C^2-2t_C\cos\gamma}\right)\left(\frac{1-tt_A}{t-t_A}\right)\left(\frac{t_C-t_A}{1-t_Ct_A}\right)\left(\frac{[-\ln c(1+t^2)]^{1/3}}{[-\ln c(1+t_C^2)]^{1/3}}\right) \times \left(\frac{[-\ln c(1+t)]^{1/3}}{[-\ln c(1+t_C)]^{1/3}}\right)\left(\frac{\mathrm{e}^{\Omega(t)}}{\mathrm{e}^{\Omega(t_C)}}\right), \tag{7.8}$$

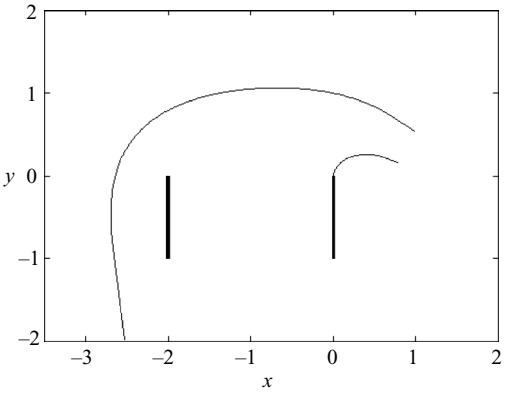

FIGURE 11. Asymmetric nozzle flow. Free-surface profiles for $\beta = 90^\circ$ and $F = 0.70$. The coordinates of the stagnation point $(x_S, y_S) = (-0.68, 1.06)$ come as part of the solution.

where $|\zeta(t_C)| = 1$. We truncate the infinite series (see (2.10)) after $N - 2$ terms and we introduce on the free surfaces the $N - 1$ mesh points

$$\sigma_M = \frac{\pi}{N-1}\left(M - \tfrac{1}{2}\right), \quad M = 1, \ldots, N-1. \tag{7.9}$$

Substituting the expressions of y and ζ into (7.1) at the mesh points σ_M, we obtain $N - 1$ nonlinear algebraic equations for the N unknowns $a_1, \ldots, a_{N-3}$, t_A, t_C and γ. The Nth equation is obtained by imposing the constraint that the two edges A and B of the nozzle have the same y, i.e.

$$y_A = y_B. \tag{7.10}$$

This system of N nonlinear equations in N unknowns is solved by Newton's method for given values of F and β using MATLAB. All the computations presented here were performed with $N = 401$. Dias & Vanden-Broeck (1990) studied similar flows, the only difference being the absence of the lower free surface on the right-hand side. They performed a detailed parametric study (influence of the Froude number and of the inclination of the nozzle on the solutions), which we do not repeat here. Instead we only provide a couple of examples in order to illustrate the extension of Dias & Vanden-Broeck's results to a jet flow on the right-hand side.

An example of a solution for an inclined nozzle is shown in figure 10(*a*). For the vertical nozzle (i.e. $\beta = 90^\circ$) case, a Froude number value of $F = 0.70$ yields the solution shown in figure 11. This solution can be compared with the symmetric case of figure 9. Moreover, it can be viewed as the juxtaposition of the nozzle flow of Dias & Christodoulides (1991) and the pouring flow of Vanden-Broeck & Keller (1986).

For a given nozzle and a given Froude number, one sees that the solution is not always unique. With the parameters of figure 11, one can have four different flows: a pouring flow on both sides, a nozzle flow on both sides, the flow shown in figure 11 and its image in a vertical mirror. But once the configuration has been imposed mathematically, the solution is unique. Which solution occurs in nature is a different question, which cannot be addressed without studying the stability of the various flows.

8. Discussion

The results presented in this paper are based on several assumptions, which we review here. First of all, the flow is assumed to be two-dimensional. A natural extension of this work would be to consider axisymmetric flows. More precisely, one could consider a nozzle with a circular cross-section and a disk for the plate. Then the flow is assumed to be incompressible. If air is entrained by the jet emerging from the nozzle, then compressible effects can play a role, especially when computing the pressure along the plate. One could use for example the basic compressible two-fluid model introduced by Dias, Dutykh & Ghidaglia (2008) and study the effect of compressibility on the flows studied here.

As stated in the introduction, the inverse problem in which one specifies the angle that the jets ought to make after hitting the plate can be investigated. For example, if one is interested in jets with constant angles, one could raise or lower the plate as the momentum of the incoming flow fluctuates inside the nozzle.

Another interesting problem is that of falling streams as opposed to rising streams. Instead of having the nozzle pointing upward, one could have a nozzle pointing downward (imagine for example figure 2 turned upside down). A question related to the inclined nozzle is: can one of the lower free surfaces ever enclose a bubble against the upper side of an inclined nozzle?

As pointed out by Raad, Chen & Johnson (1995), free-surface flows such as those presented in this paper can be used to validate numerical codes for two-dimensional, unsteady, incompressible, free-surface fluid flows. Indeed, these types of flows are notoriously difficult to compute. In impact problems, variations in time play an important role. Cooker & Peregrine (1995) studied the high pressures and sudden velocity changes which may occur in the impact between a region of incompressible liquid and a solid surface. Their theory rests upon the idea of pressure impulse, for the sudden initiation of fluid motion in incompressible fluids. Results were obtained for the peak pressure distribution and the velocity after impact.

The authors are grateful for a number of helpful comments from J.-M. Vanden-Broeck. This research was partially supported by the Bilateral-cooperation Program between Cyprus and France of the Cyprus Research Promotion Foundation under the project CY-FR/0305/09 and the Zenon Program of the French Ministry of Foreign Affairs under the project 12089ZB.

REFERENCES

Clanet, C. 1998 On large-amplitude pulsating fountains. *J. Fluid Mech.* **366**, 333–350.

Cooker, M. J. & Peregrine, D. H. 1995 Pressure-impulse theory for liquid impact problems. *J. Fluid Mech.* **297**, 193–214.

Dias, F. & Christodoulides, P. 1991 Ideal jets falling under gravity. *Phys. Fluids* A **3**(7), 1711–1717.

Dias, F., Dutykh, D. & Ghidaglia, J.-M. 2008 A two-fluid model for violent aerated flows, preprint.

Dias, F., Keller, J. & Vanden-Broeck, J.-M. 1988 Flows over rectangular weirs. *Phys. Fluids* **31**, 2071–2076.

Dias, F. & Tuck, E. O. 1991 Weir flows and waterfalls. *J. Fluid Mech.* **230**, 525–539.

Dias, F. & Vanden-Broeck, J.-M. 1990 Flows emerging from a nozzle and falling under gravity. *J. Fluid Mech.* **213**, 465–477.

Dias, F. & Vanden-Broeck, J.-M. 1993 Nonlinear bow flows with spray. *J. Fluid Mech.* **255**, 91–102.

Goh, K. H. M. & Tuck, E. O. 1985 Thick waterfalls from horizontal slots. *J. Engng Math.* **19**, 341–349.

Hureau, J., Brunon, E. & Legallais, P. H. 1996 Ideal free streamline flow over a curved obstacle. *J. Comput. Appl. Math.* **72**, 193–214.

Milne-Thomson, L. M. 1996 *Theoretical Hydrodynamics* (5th ed.). Dover Publications.

Peng, W. & Parker, D. F. 1997 An ideal fluid jet impinging on an uneven wall. *J. Fluid Mech.* **333**, 231–255.

Raad, P. E., Chen, S. & Johnson, D. B. 1995 The introduction of micro cells to treat pressure in free surface fluid flow problems. *J. Fluid Engng Trans. ASME* **117**, 683–690.

Tuck, E. O. 1987 Efflux from a slit in a vertical wall. *J. Fluid Mech.* **176**, 253–264.

Vanden-Broeck, J.-M. 1993 Two-dimensional jet aimed vertically upwards. *J. Austral. Math. Soc. Ser.* B **34**, 393–400.

Vanden-Broeck, J.-M. & Keller, J. B. 1982 Jets rising and falling under gravity. *J. Fluid Mech.* **124**, 335–345.

Vanden-Broeck, J.-M. & Keller, J. B. 1986 Pouring flows. *Phys. Fluids* **29**, 3958–3961.

Vanden-Broeck, J.-M. & Keller, J. B. 1987 Weir flows. *J. Fluid Mech.* **176**, 283–293.

Wiryanto, L. H. & Tuck, E. O. 2000 An open-channel flow meeting a barrier and forming one or two jets. *J. Austral. Math. Soc. Ser.* B **41**, 458–472.